*International Journal of Thermophysics, Vol. 21, No. 3, 2000*

# A Nonclassical Model of a Type 2 Mixture with Vapor–Liquid, Liquid–Liquid, and Three-Phase Equilibria

**J. C. Rainwater**[1]

A model with nonclassical exponents is developed for phase equilibria of a Type 2 mixture with vapor–liquid equilibrium (VLE) and liquid–liquid equilibrium (LLE). Starting with a Leung–Griffiths model for a Type 1 mixture with only VLE, the model adds a Schofield parametric construction to describe LLE and a three-phase locus. Care is taken to suppress a spurious and artificial phase boundary. The model is applied to VLE data of carbon dioxide + methane. It is conjectured that this mixture upon cooling would undergo liquid–liquid separation, but it freezes before such "virtual LLE" can be observed. Experimental bubble curves and the LLE structure from a classical equation of state are accurately modeled.

**KEY WORDS:** carbon dioxide; critical exponents; liquid–liquid equilibria; methane; three-phase locus; Type 2 mixture; vapor–liquid equilibria.

## 1. INTRODUCTION

Van Konynenburg and Scott [1] have shown that the phase diagram of a binary mixture can exhibit one of six types of topological structure. In the simplest case, Type 1, the only coexisting fluid states are vapor–liquid equilibria (VLE). In Type 2, the next simplest, the mixture additionally displays liquid–liquid equilibria (LLE), with two distinct critical loci, a plait-point locus for VLE and a consolute-point locus for LLE. The VLE and LLE surfaces intersect along a three-phase liquid–liquid–vapor (LLV) locus that terminates in an upper critical end point (UCEP).

Cubic equations of state such as the Peng–Robinson equation [2] can describe the first five types of phase diagrams, and more complex equations

[1] Physical and Chemical Properties Division, Chemical Science and Technology Laboratory, National Institute of Standards and Technology, Boulder, Colorado 80303, U.S.A.



0195-928X/00/0500-0719$18.00/0 

can yield the sixth type [3]. However, phase boundaries as calculated from analytic equations of state are always described by (incorrect) classical critical exponents. For example, if $\Delta\rho$ is the liquid–vapor density difference of a pure fluid, then within the near-critical region,

$$\Delta\rho = C_\rho(-t)^\beta \tag{1}$$

where $C_\rho$ is a constant, and $t = (T - T_c)/T_c$, where $T$ is temperature and $T_c$ is critical temperature. Similarly, for binary mixture LLE on an isobaric plane, the composition change $\Delta x$ between coexisting liquid states goes as

$$\Delta x = C_x(-t)^\beta \tag{2}$$

Critical-region thermodynamics is characterized by two and only two independent critical exponents, which can be taken to be $\alpha$ (which characterizes the divergence of constant-volume specific heat) and $\beta$. The theory of critical exponents is by now well developed [4]. In this work we use simple scaling [the single nonanalytic term in Eq. (1)] and effective exponents ($\beta = 0.355$, $\alpha = 0.1$) that fit thermodynamic behavior better over a wider range than theoretical exponents ($\beta = 0.325$, $\alpha = 0.11$) but are much closer to theoretical than to classical exponents ($\beta = 0.5$, $\alpha = 0$).

The Leung–Griffiths model [5], as modified by Moldover, Rainwater, and co-workers [6–8] and with effective exponents, has proven useful for accurate correlation of VLE surfaces for many Type 1 mixtures [9]. A version of the model with a crossover function and theoretical exponents has been developed [10], but such refinements are not used in the present work. Similar nonclassical models have been developed for LLE [11–13], but only on an isobaric plane. More recently, Cheng et al. [14] have modeled nonclassically the Type 5 mixture methane + *n*-hexane and the smooth transition from VLE to LLE along the upper branch of the critical locus, but not the coexisting vapor along the liquid–liquid–vapor three-phase locus. In this work, we develop a nonclassical model of a Type 2 mixture with VLE and LLE surfaces joined by a three-phase LLV locus, all of which are described by effective nonclassical critical exponents and with the proper derivative discontinuities in the vapor-phase boundaries.

## 2. THE NONCLASSICAL TYPE 2 MODEL

Griffiths and Wheeler [15] have shown that the thermodynamic surfaces of mixtures can be described in terms of field variables such as pressure $P$, temperature $T$, chemical potential $\mu_i$, and functions thereof, which by definition are continuous across a phase boundary. For binary mixtures, the thermodynamic surface may be described in terms of one

(arbitrarily chosen) dependent field variable or "potential" as a function of three independent field variables. The potential is a continuous function of the independent fields but has manifolds of discontinuities in derivatives that represent phase boundaries. Density variables such as $\rho$ and $x$, which by definition differ across phase boundaries, are then partial derivatives of the potential with respect to the independent fields.

In principle, therefore, all types of mixture phase diagrams can be described by multidimensional, continuous functions with manifolds of derivative discontinuities to describe the phase boundaries. The approach taken here is to construct such functions. Our Type 2 mixture model is based on the Leung–Griffiths [5] model of Type 1 mixtures, which in turn is based on the Schofield [16] model of pure fluids. In the variant of the Schofield model used by Leung and Griffiths, the potential $\omega = P/RT$ (where $R$ is the gas constant) is a function of $t$ (defined earlier) and $h$:

$$h = \ln(e^{\mu_1/RT} + Ke^{\mu_2/RT}) - H \to \mu_1 - \mu_1^0 \tag{3}$$

$$H = \ln(e^{\mu_1^\sigma/RT} + Ke^{\mu_2^\sigma/RT}) \to \mu_1^0 \tag{4}$$

Here the superscript s denotes the value on the coexistence surface, and $K$ can be a constant or a temperature-dependent function [17]; more general dependences have also been considered [10]. The arrows denote the limit of pure fluid 1 in a binary mixture of fluids 1 and 2. The potential with a phase boundary is described parametrically in terms of new variables $r$ and $\theta$ as

$$\omega = \omega_{\text{reg}} + \omega_{\text{VLE}} = \omega_{\text{reg}} + C_\omega G(r, \theta) \tag{5}$$

$$G(r, \theta) = r^{2-\alpha}[a_0 + a_2\theta^2 + a_4\theta^4] \tag{6}$$

$$t = r(1 - b^2\theta^2)/(b^2 - 1) \tag{7}$$

$$h = C_h r^{2-\alpha-\beta}\theta(1 - \theta^2) \tag{8}$$

where $\omega_{\text{reg}}$ is a background term analytic in its field variable arguments, $C_\omega$ and $C_h$ are fluid-dependent constants, and $a_0$, $a_2$, $a_4$, and $b$ are functions of the critical exponents [8]. The phase boundary is $h = 0$, $t < 0$, the liquid side is $\theta = 1$, and the vapor side is $\theta = -1$. A thermodynamic analysis [5] shows that the molar density $\rho$ is

$$\rho = (\partial\omega/\partial h)_t \tag{9}$$

The potential described by Eqs. (5)–(8) is continuous everywhere including the phase boundary, but at that boundary its derivative, Eq. (9), is discontinuous, with liquid density at $\theta = 1$ or as $h \to 0$ from above, and vapor

density at $\theta = -1$ or as $h \to 0$ from below. It is straightforward to show that Eq. (1) is obeyed, with $C_\rho = 2C_\omega/C_h$.

Leung and Griffiths generalized the pure-fluid Schofield model to Type 1 binary mixtures by means of the "hidden" or "spectator" variable $\zeta$, where

$$\zeta = e^{\mu_1/RT}/(Ke^{\mu_2/RT} + e^{\mu_1/RT}) \tag{10}$$

which can be interpreted as a field-variable analog of composition $x$, a density variable. In the Leung–Griffiths model, $C_\omega$ and $C_h$ are functions of $\zeta$, which is held constant in Eq. (9). The background $\omega_{\text{reg}}$ is analytic in $\zeta$, $t$, and $h$. With $\omega_{\text{VLE}}$ accurately describing the changes in $\rho$ and $x$ across the phase boundary, sufficient parameters are introduced into the background $\omega_{\text{reg}}$ so that actual VLE surfaces can be accurately correlated [9]. In terms of the independent field variables, the coexistence locus of the more volatile fluid is $\zeta = 0$, $h = 0$, $t < 0$, and that of the less volatile fluid is $\zeta = 1$, $h = 0$, $t < 0$. The plait-point locus is $0 < \zeta < 1$, $t = 0$, $h = 0$ and the VLE surface is $0 < \zeta < 1$, $t < 0$, $h = 0$.

In a typical Type 2 mixture $P$–$T$ phase diagram, the three-phase locus is roughly parallel to, and slightly below, the vapor pressure curve of the more volatile component, and that locus terminates in an UCEP. The consolute-point locus usually is nearly independent of pressure, so it rises from the UCEP vertically.

Figure 1 shows the phase boundaries in three-dimensional $P$–$T$–$\zeta$ space. The LLE surface is approximately a perpendicular plane that is bounded from above in temperature by the consolute point locus. That surface cuts into the VLE surface along a three-phase locus, bounded from above in temperature by the UCEP. Because of the 180° rule as analyzed by Wheeler [18], the presence of LLE distorts the VLE surface. As shown, along the three-phase locus the VLE surface develops an upward crease (derivative discontinuity), where the sharpness of the crease (magnitude of derivative discontinuity) increases with distance from the UCEP according to the exponent $\beta$. To construct the Type 2 model, we first place the UCEP at $h = 0$, $t = t_0$, $\zeta = \zeta_0$, where $t_0 < 0$ and $0 < \zeta_0 < 1$. A term is then added to the potential, Eq. (5), to describe LLE:

$$\omega = \omega_{\text{reg}} + \omega_{\text{VLE}} + \omega_{\text{LLE}} \tag{11}$$

$$\omega_{\text{LLE}} = C_{\text{L}}[G(\bar{r}, \bar{\theta}) + \omega_{\text{corr}}] \tag{12}$$

$$\bar{\zeta} = s_\zeta^{-1}(\zeta - \zeta_0) = \bar{r}^{2-\alpha-\beta}\bar{\theta}(1 - \bar{\theta}^2) \tag{13}$$

$$\bar{t} = s_t^{-1}(t - t_0) = \bar{r}(1 - b^2\bar{\theta}^2)/(b^2 - 1) \tag{14}$$

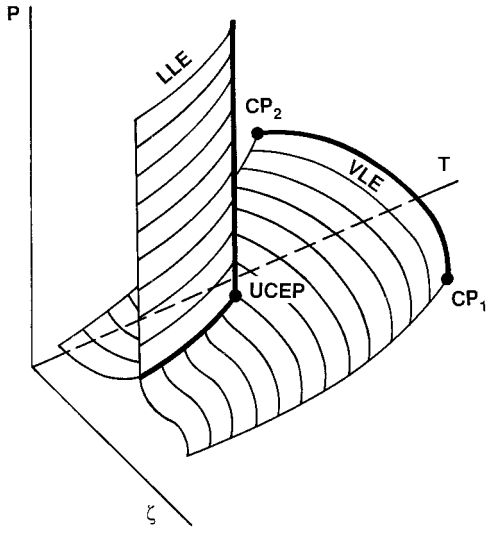


**Fig. 1.** Three-dimensional $P$–$T$–$\zeta$ diagram of the phase boundaries of a Type 2 mixture. The pure fluid critical points are labeled $CP_1$ and $CP_2$. The curved VLE surface is intersected by the LLE surface, approximately a vertical plane, along a three-phase locus that terminates at the UCEP. The VLE surface has a crease along the three-phase locus, as shown.

Here $\omega_{\text{corr}}$ is an analytic correction term, included so that boundary conditions are obeyed, and $C_L$, $s_\zeta$, and $s_t$ are scale factors. The above construct yields a consolute point locus at $\zeta = \zeta_0$, $t = t_0$, $h > 0$, which complies with the approximation of a pressure-independent locus. The three-phase locus is $h = 0$, $\zeta = \zeta_0$, $t < t_0$, and the LLE surface is $h > 0$, $\zeta = \zeta_0$, $t < t_0$, across which $x_\ell$, the liquid composition, is discontinuous. We note that, for LLE, $\bar{t}$ and $\bar{\zeta}$ play the roles for VLE of $t$ and $h$, respectively, and for LLE, $h$ (instead of $\zeta$) is the spectator variable. $C_L$ and $s_\zeta$ could be made functions of $h$ in Eqs. (12) and (14), but in the initial model they are constants, so that the added LLE terms do not affect the liquid and vapor densities. Actually, in the final model, an $h$-dependent term must be added to $\omega_{\text{LLE}}$, but this will be introduced and justified later.

Scaling-law models in general for binary mixtures are characterized by a strong field $h_1$, a weak field $h_2$, and a hidden or spectator field [19]. The strong field is conjugate to an order parameter, which for the pure-fluid vapor–liquid transition is the density. Scaling-law behavior is described by nonanalytic functions of the strong and weak fields with coefficients

analytically dependent on the hidden field. In our model, within the VLE construct $h$ is the strong field, $t$ is the weak field, and $\zeta$ is the hidden field, while in the LLE construct these fields are, respectively, $\bar{\zeta}$, $\bar{t}$, and $h$.

Due to the complexity of the present problem, we have constructed this initial model at the level of simple scaling. In revised scaling models [20, 21] for pure fluids and mixtures, the strong field is $h$ with a small linear admixture of $t$, and the weak field is $t$ with a small linear admixture of $h$. Similar mixing of variables could be introduced for LLE in extensions of this model, but with resulting mathematical complications.

Anisimov et al. [19] have examined the structure of scaling-law models for general phase behavior in binary mixtures. The most general forms for the strong and weak fields are

$$h_1 = a_1 \Delta\mu_1 + a_2 \Delta T + a_3 \Delta\mu \tag{15}$$

$$h_2 = b_1 \Delta T + b_2 \Delta\mu_1 + b_3 \Delta\mu \tag{16}$$

where $\Delta T = T - T_c$, $\Delta\mu_1 = \mu_1 - \mu_{1c}$, $\mu = \mu_2 - \mu_1$, and $\Delta\mu = \mu - \mu_c$.

In the present model $t$ is a dimensionless form of $\Delta T$, $\zeta$ is a function of $\mu$, and for small $x$, $\mu_1$ behaves somewhat like $h$. Anisimov et al. show that, for VLE in the limit of small $x$, $a_3 = b_3 = 0$ and $\mu$ (or equivalently $\zeta$) is the hidden variable, while for LLE in the incompressible limit $a_1 = b_2 = 0$ and $\mu_1$ is the hidden field, in correspondence with our LLE construct in which $h$ is the hidden field.

Anisimov et al. [19] also consider a Type 5 binary mixture, where the critical locus has two branches. The branch starting from the critical point of the less volatile component begins as a locus of VLE critical points, but as the temperature is reduced it gradually turns into a locus of LLE critical points until it reaches a critical end point. They define an angle $\phi$ as

$$\phi = \tan^{-1}(a_3/a_1) \tag{17}$$

and show that $\phi = 0$ at the critical point of the less volatile pure fluid but continuously changes to $\phi = \pi/2$ at the critical end point. Similarly, our VLE and LLE constructs can be viewed as differing by a rotation of 90° in field variable space.

It is our objective to describe the phase boundary surface of a Type 2 mixture in full, including the three-phase locus, over an extended critical region. Cheng et al. [14] have applied the formalism of Anisimov et al. [19] to study the Type 5 mixture methane + *n*-hexane. They obtain good agreement with the liquid–liquid phase boundaries near the critical end point. In $P$–$T$–$\zeta$ space, the full Type 5 boundary surface can be illustrated

similarly to Fig. 1 for the Type 2 surface, but with a single continuous surface that folds onto itself along a three-phase locus bounded by critical end points at both ends. Unlike the present work, Cheng et al. do not consider a mathematical description of the three-phase locus or the vapor phase in coexistence with the liquid phases at the critical end point.

## 3. SUPPRESSION OF SPURIOUS PHASE BOUNDARIES

Without further refinement, the model as constructed to this point describes a discontinuity in $x$ within the vapor part of the phase diagram $h<0,\ \zeta=\zeta_0,\ t<t_0$. In other words, it incorrectly includes a completely spurious and artificial "vapor–vapor equilibrium" within a region that physically is a completely miscible binary gas mixture.

In the present model, the independent fields $\zeta$ and $h$ are still defined according to Eqs. (3), (4), and (10), and the superscript $\sigma$ in Eq. (4) still represents the value on the (now creased) VLE surface. Consequently, surfaces of constant $h>0$ in the liquid region and $h<0$ in the vapor region also display such a crease. In the one-phase vapor regime, although $\omega$ must be continuous and differentiable in standard field variables (e.g., $T, \mu_1$, and $\mu_2$), derivatives such as $(\partial\omega/\partial\zeta)_h$ will have discontinuities at $\zeta=\zeta_0$ because $h$ and $H$ possess discontinuous derivatives with respect to the standard field variables.

Within the Leung–Griffiths model, composition is given by

$$x=1-\zeta-\zeta(1-\zeta)\left\{\rho^{-1}\left[\left(\frac{\partial\omega}{\partial\zeta}\right)_{t,h}+\frac{1}{B_c}\frac{dB_c}{d\zeta}(1+t)\left(\frac{\partial\omega}{\partial t}\right)_{\zeta,h}\right]\right.$$
$$\left.-\left(\frac{\partial H}{\partial\zeta}\right)_t-\frac{1}{B_c}\frac{dB_c}{d\zeta}(1+t)\left(\frac{\partial H}{\partial t}\right)_{\zeta,h}\right\} \tag{18}$$

where $B_c=1/RT_c$. For $h=0$, substitution of $\rho_\ell$ or $\rho_v$ (where subscripts $\ell$ and v denote liquid and vapor) into Eq. (18) yields $x_\ell$ or $x_v$, respectively. Also, in previous applications of the Leung–Griffiths model, it has been assumed that $H(\zeta, t)$, or in the modified version [6–9] a closely related function, $\bar{H}(\zeta, t)$, can be modeled independently of $\omega(\zeta, t, h)$. For the inclusion of LLE, we not only modify $\omega$ but also $H$, which is done as follows:

$$\begin{aligned}\rho_b(t)&=\rho_v(\zeta_0, t), && t<t_0\\ \rho_b(t)&=\rho_0+\rho_1\bar{t}+\rho_2\bar{t}^2, && t>t_0\end{aligned} \tag{19}$$

$$H_{LLE}(\zeta, t)=|\rho_b(t)|^{-1}\,C_L\,G(\bar{r}, \bar{\theta}) \tag{20}$$

$$H(\zeta, t)=H_{VLE}(\zeta, t)+H_{LLE}(\zeta, t) \tag{21}$$

where $\rho_0$, $\rho_1$, and $\rho_2$ are chosen so that the value and first two derivatives of $\rho_b$ are continuous. With this modification, according to Eq. (18), along a locus of constant $t < t_0$ on the vapor side of the VLE surface there is no discontinuity in $x_v$, but there is a discontinuity on the liquid side in $x_\ell$ at $\zeta = \zeta_0$. This discontinuity describes LLE, as desired. By this technique, we have suppressed "vapor–vapor equilibria" on the phase boundary, which is our primary interest, but we have not necessarily done so throughout the one-phase vapor region. We return to this point in Section 5.

## 4. ADJUSTABLE UCEP AND STRETCHING FUNCTION

In the implementation of the model, while the temperature and pressure of the UCEP are determined from experiment, the values of $t_0$ and $\zeta_0$ for the UCEP are in general not a priori known. Thus, it is useful to construct a correlation method so that the position of the UCEP can be adjusted as necessary.

We first construct $\omega_{LLE}$ from Eqs. (12)–(14) for the choices $t_0 = -0.075$, $\zeta_0 = 0.1$, and $s_t = s_\zeta = 1$. Since the usual range of the modified Leung–Griffiths model is $-0.1 < t < 0$, this choice of $t_0$ is toward the lower end of but within that range, while the choice of $\zeta_0$ is based on the observation that the three-phase locus is typically close to the vapor pressure curve of the more volatile component and therefore should be closer to 0 than to 1. We evaluate $G(\bar{r}, \bar{\theta})$ along the loci $\bar{t} = 0.075$ and $\bar{\zeta} = -0.1$, fit those functions to polynomials in $\bar{\zeta}$ and $\bar{t}$, respectively, and then construct a product of those polynomials in $\bar{\zeta}$ and $\bar{t}$ that thereby fits $G(\bar{r}, \bar{\theta})$ along the two loci, and, finally, choose $\omega_{corr}$ to be the negative of this polynomial. Except for small fitting errors, $\omega_{LLE}$ is then zero along the plait point locus, $t = 0$, and the coexistence locus of the volatile component, $\zeta = 0$.

We then make a simple linear transformation of the independent variables with scale factors $s_t$ and $s_\zeta$,

$$t_0 = 0.075 s_t \tag{22}$$

$$\bar{t} = (t - t_0)/s_t = \bar{r}(1 - b^2\bar{\theta}^2)/(b^2 - 1) \tag{23}$$

$$\zeta_0 = 0.1 s_\zeta \tag{24}$$

$$\bar{\zeta} = s_\zeta^{-1}(\zeta - \zeta_0) = \bar{r}^{2-\alpha-\beta}\bar{\theta}(1 - \bar{\theta}^2) \tag{25}$$

This transformation retains the constraint that, within fitting error, $\omega_{LLE}$ is zero for $h = 0$ on the plait-point locus, $t = 0$, and the coexistence curve of the volatile fluid, $\zeta = 0$. From the symmetry of the function $G(\bar{r}, \bar{\theta})$, $\omega_{LLE}$ also vanishes along the locus $\zeta = 0.2 s_\zeta$, but we want it instead to

vanish along the coexistence curve of the nonvolatile fluid, i.e., $\zeta = 1$. In other words, the LLE construct must be changed from symmetric to asymmetric, which we accomplish by the variable transformation:

$$\zeta'/s_\zeta = \bar{\zeta} + a\{\exp[(\bar{\zeta} - \zeta_S)/a] - \exp(-\zeta_S/a)\} \tag{26}$$

where $a$ and $\zeta_S$ are constants, and change the first equality of Eq. (13) to

$$\zeta = \zeta' + \zeta_0 \tag{27}$$

From Eq. (26), we have

$$s_\zeta \, d\bar{\zeta}/d\zeta' = \{1 + \exp[(\bar{\zeta} - \zeta_S)/a]\}^{-1} \tag{28}$$

which has the form of a Fermi–Dirac distribution function. For small $a$, the derivative is close to one for $\bar{\zeta} < \zeta_S - a$ and close to zero for $\bar{\zeta} > \zeta_S + a$. In order for $\omega_{\mathrm{LLE}}$ to vanish on the coexistence curve of the nonvolatile fluid, we require that $\zeta = 0.9$ when $\bar{\zeta} = 0.1 s_\zeta$, a constraint that determines $\zeta_S$ in Eq. (26) for a given choice of $a$. Thus we have introduced a one-parameter "stretching transformation" that transforms the interval $0 < \zeta < 2\zeta_0$ into the interval $0 < \zeta < 1$. Since the LLE construct should distort the VLE phase boundary near $\zeta = \zeta_0$, but not near $\zeta = 1$ (mixtures rich in the nonvolatile component), we have found it useful to replace Eq. (21) by

$$H_{\mathrm{LLE}}(\zeta, t) = [\rho_{\mathrm{b}}(t)]^{-1} \, C_{\mathrm{L}} G(\bar{r}, \bar{\theta}) \, s_\zeta \, d\bar{\zeta}/d\zeta' \tag{29}$$

which leaves the model essentially unchanged near $\zeta = \zeta_0$ since in that region $s_\zeta \, d\bar{\zeta}/d\zeta' \approx 1$. If the original Leung–Griffiths thermodynamic potential ($\omega_{\mathrm{reg}} + \omega_{\mathrm{VLE}}$) is fitted to the pure-fluid coexistence curves and the plait point locus, the addition to that potential, $\omega_{\mathrm{LLE}}$, vanishes along (and thus retains the model fit to) those three loci while adding the new phase transition of LLE to the thermodynamic description.

## 5. VAPOR DENSITY AUGMENTATION

While during the development of this formalism, it was initially hoped that the LLE part of the potential could be made independent of $h$, as in Eqs. (12)–(14). Further analysis showed that some $h$-dependence must be introduced in a specific and careful manner. The problem is that "vapor–vapor equilibria" must be suppressed not only on the phase boundary (as it has in the model as described to this point), but also within the one-phase vapor region away from the boundary. Let $\Delta\omega_\zeta$ and $\Delta H_\zeta$ be the

amounts of discontinuity in $\partial\omega/\partial\zeta$ and $\partial H/\partial\zeta$, respectively, along the surface $\zeta = \zeta_0$, $t < t_0$. We require, not just for $h = 0$, but also for all $h < 0$, that

$$\Delta\omega_\zeta(t, h) = \rho\, \Delta H_\zeta(t, h) \tag{30}$$

Upon considering a small increment of distance into the one-phase vapor region (small negative $h$), we find that

$$\left(\frac{\partial\omega_{\mathrm{LLE}}}{\partial h}\right)_{\zeta,\, t} = \rho_{\mathrm{LLE}} = H_{\mathrm{LLE}} \left(\frac{\partial\rho}{\partial h}\right)_{\zeta,\, t} \tag{31}$$

where $\rho_{\mathrm{LLE}}$ is the contribution from $\omega_{\mathrm{LLE}}$ to the vapor density $\rho$. From the description to this point, such a contribution is zero. Also, as we increase the magnitude of negative values of $h$, and thus move from the phase boundary into the one-phase vapor region, $\rho$ must decrease and thus $\partial\rho/\partial h$ is positive. The model to this point is thus inconsistent in that the left side of Eq. (31) is zero, and consequently we must introduce some $h$-dependence into $\omega_{\mathrm{LLE}}$. Because of the way it was defined, the variable $H$ cannot have any $h$-dependence.

There are constraints that need to be obeyed. The full $\omega$ must be a field variable, continuous in $\zeta$, $t$, and $h$. Since we already have a VLE transition we may add to the discontinuity in $\partial\omega/\partial h$ for $t < 0$, but there must be no discontinuity for $t > 0$. We must avoid the introduction of any spurious phase transitions by means of derivative discontinuities away from the VLE and LLE surfaces. Finally, we want our modification not to disturb the fit to the vapor pressure and coexisting density curves of the pure components or the fit to the plait-point locus. A modification of Eq. (12) that accomplishes these objectives is

$$\omega_{\mathrm{LLE}} = C_{\mathrm{L}}[\, G(\bar{r}, \bar{\theta}) + \omega_{\mathrm{corr}}] \left\{1 + C_{\mathrm{VC}} h\Theta(-h)(1 - \bar{\zeta}^2/0.001)\, e^{t_{\mathrm{r}}/t} \left(1 + \frac{t}{2t_{\mathrm{r}}}\right)\right\}$$

$$\text{if} \quad t < 0$$

$$\omega_{\mathrm{LLE}} = 0 \qquad \text{if} \quad t > 0 \tag{32}$$

where $\Theta(h)$ is the Heaviside step function. This introduces two additional parameters, a characteristic reduced temperature $t_{\mathrm{r}}$ and an amplitude $C_{\mathrm{VC}}$. The exponential form ensures that the function and all derivatives are continuous at the plait-point locus $t = 0$, and the $\zeta$ dependence leaves the thermodynamic potential unchanged on the pure-fluid coexistence curves $\zeta = 0$ and $\zeta = 1$.

This modification leaves the liquid density unchanged but increases the vapor density since, as explained above, $C_{VC}$ must be positive and

$$\rho_{LLE} = C_{VC}\omega_{LLE}(\zeta_0, t)(1 - \bar{\zeta}^2/0.01)(1 + t/2t_r)\exp(t_r/t) \tag{33}$$

The increase in vapor density generally leads to an increase in vapor composition of the volatile component, and its introduction has led to significant improvement in the correlation of our test mixture. Except for the relation between $x$ and $\zeta$ on the plait-point locus, this completes the description of our nonclassical Type 2 mixture model.

## 6. APPLICATION TO CARBON DIOXIDE + METHANE

For an initial candidate system to test our model, we searched for a binary mixture with extensive VLE data in the critical region and with LLE limited by a UCEP not far from the plait-point locus. We also sought a mixture for which classical equations of state are available [22]. Without that condition, from the experimental literature the best choices appear to be carbon dioxide + carbon disulfide [23] and water + sulfur dioxide [24]. However, carbon disulfide and sulfur dioxide are not included in the available NIST14 computer package.

As an alternative, we chose the mixture carbon dioxide + methane. Although this mixture does not exhibit LLE in nature, there is evidence that, on cooling, it would liquid–liquid separate except that it freezes first. Figure 2 shows the plait-point locus and VLE data from a number of sources [25–29] for this mixture. The isotherms from 193.15 to 210.15 K terminate as the pressure is lowered on a three-phase solid–liquid–vapor locus that has been measured in detail [30].

Figure 2 also shows an earlier attempt to correlate the VLE data of this mixture [9]. As earlier noted by Al-Sahhaf et al. [31], the modified Leung–Griffiths model does not quantitatively describe the phase boundary. The isotherms at the highest temperatures are described well, and it is in this region that classical equations of state do not do as well and deviate noticeably from experiment [32, 33]. However, on the methane-rich side, the dew-bubble curves are predicted to be much too narrow.

It was this behavior, in stark contrast to the success of the model for most other similar mixtures, that originally motivated the present study [9]. Similar discrepancies for carbon dioxide + methane have been found with a scaling-law model and the extended corresponding states approach of Kiselev and Rainwater [34]. One problem is that critical-region densities have been measured only at the carbon-dioxide-rich end [25, 35], and while our choice of critical density locus agrees well with experimental

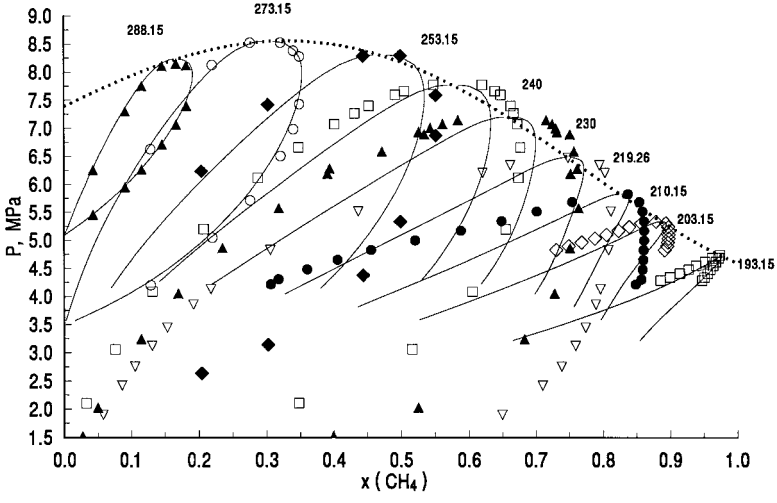


**Fig. 2.** VLE surface of carbon dioxide + methane in $P$–$x$ space. Experimental isotherms are from Refs. 25–29 with temperatures in K, as shown. The dotted line is the critical locus and solid lines are isothermal dew-bubble curves from the modified Leung–Griffiths model.

coexisting densities, it does show some peculiar behavior at the methane-rich end, such as an unusual negative excess compressibility factor [34]. However, in the absence of data, we did not try to adjust the critical density locus in that region.

The partially conjectured phase diagram of carbon dioxide + methane is shown in Fig. 3. If freezing could be suppressed, our hypothesis is that the mixture would display a three-phase locus with a UCEP and a critical locus for LLE (consolute point locus), all of which are labeled "virtual" in Fig. 3. In Fig. 2, an inflection point can be seen on the bubble curve of Mraw et al. [28] at 210.15 K, which is a characteristic of phase diagrams of Type 2 mixtures. As the temperature is lowered, the slope of the curve at the inflection point decreases until that slope is horizontal at the UCEP, below which there are tie lines for LLE. This pattern of inflection points is clear in the Peng–Robinson correlation of carbon dioxide + methane of Knapp et al. [36].

From the NIST14 program [37], after a warning message for freezing is suppressed, LLE is found with a UCEP at $T = 181.95$ K, $P = 2.665$ MPa, and $x = 0.5$. Miller and Luks [38] have studied UCEP locations for the family of carbon dioxide + $n$-alkane mixtures above and including $n$-heptane. For a carbon number of less than seven, the extrapolated UCEP is below the freezing locus, although Im and Kurata [39] were able to

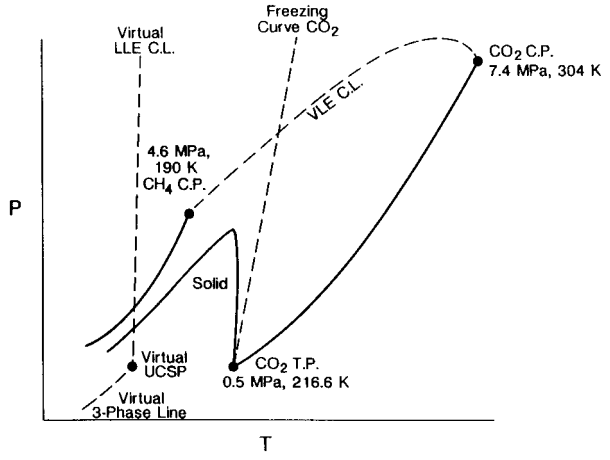


**Fig. 3.** Partially conjectured $P$–$T$ phase diagram for carbon dioxide + methane (schematic), with vapor-pressure curves, plait-point locus, and solid–liquid–vapor locus [9]. Our conjecture is that, if freezing were suppressed, this mixture would show consolute-point and three-phase LLV loci as shown.

observe LLE in a supercooled mixture of carbon dioxide + *n*-hexane. If the UCEP locus in Fig. 3 of Miller and Luks is extrapolated to a carbon number of one, a temperature of about 180 K is obtained, consistent with the prediction of NIST14. This liquid–liquid separation is too far below the freezing locus to be observable experimentally even by supercooling, but its presence in the fluid solution of the thermodynamics is expected to distort the VLE phase boundaries.

The three-phase locus may be mapped with NIST14 for a series of fixed vapor compositions and by variation of the input pressure. It is found that the composition of the coexisting liquid changes discontinuously at a specific pressure, which determines the mole fractions of the two coexisting liquids. The three-phase locus predictions of NIST14 are shown as gray circles in Fig. 4; these results obey Eq. (2), but, as expected from a classical equation of state, $\beta = 0.5$. The present model, in contrast, yields an effective scaling-law exponent of $\beta = 0.355$.

Our objective is to adjust the parameters of our model with LLE so that, to the extent possible, we describe both the experimental VLE data and the three-phase locus predictions of NIST14. We also want our correlation to be consistent with the 180° rule, as described by Wheeler [18]. As an isotherm crosses the three-phase locus, while the liquid composition is discontinuous, the vapor composition is continuous but with a discontinuous derivative $dP/dx$, so that there is a sharp corner on the dew

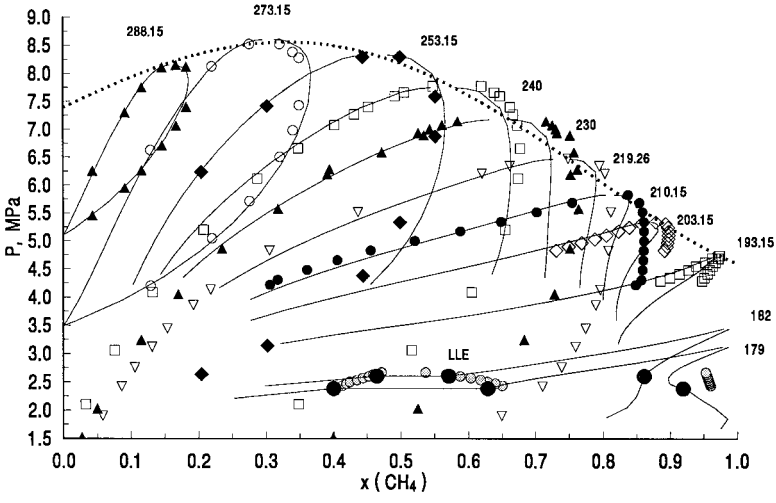


**Fig. 4.** VLE surface of carbon dioxide + methane in $P$–$x$ space. Experimental isotherms from Refs. 25–29, with temperatures in K, as shown. Solid lines are phase boundaries of present model. At lower temperatures, the data terminate on a solid–liquid–vapor locus, below which the model predicts LLE. Gray circles denote a classical LLE structure as calculated from Ref. 37. Large, filled dark circles are three-phase LLV points of the model.

curve. Also, according to the 180° rule, as an arrow this corner must point from the one-phase toward the multiphase region [18].

We found, with some disappointment, that the inclusion of the LLE potential did not significantly increase the calculated widths of the dew-bubble curves. To reproduce those widths, we followed a procedure used earlier for the azeotropic mixture ethane + hydrogen sulfide [9]. We define $w_r$ as the ratio of theoretical to experimental dew-bubble curve widths according to the modified Leung–Griffiths model with the critical line condition [17] $x = 1 - \zeta$ on the plait-point locus. We then seek to reproduce the experimental widths by changing from linear the relation between $\zeta$ and $x$ on that locus. The desired relation $\zeta(x_1)$ on that locus, where $x_1 = 1 - x$, then satisfies the differential equation:

$$\frac{d\zeta}{\zeta(1-\zeta)} = \frac{dx_1}{x_1(1-x_1)}\, w_r(x_1) \tag{34}$$

and, from theoretical considerations [9],

$$w_r(x_1) = 1 + x_1(1-x_1)\, w_E(x_1) \tag{35}$$

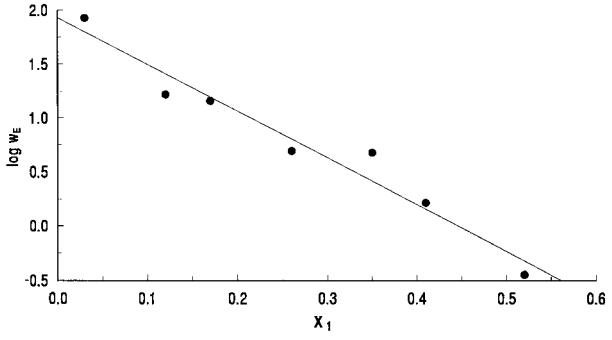


**Fig. 5.** Semilogarithmic plot of $w_E$, determined from Fig. 1, as a function of $x_1$, and fit to Eq. (37).

where $w_E(x_1)$ is finite and, in this example, negative. The solution to Eq. (34) is then

$$\zeta(x_1) = \frac{Cx_1 \exp[\int_0^{x_1} w_E(x_1')\, dx_1']}{1 - x_1 + Cx_1 \exp[\int_0^{x_1} w_E(x_1')\, dx']} \tag{36}$$

where $C$ is a constant of integration.

The function $w_E(x_1)$, as determined from graphical observation of Fig. 2, is displayed in the semilogarithmic plot in Fig. 5. The approximately straight line behavior indicates that

$$w_E = C_{W1} e^{-C_{W2} x_1} \tag{37}$$

We used the form of Eq. (37), but with subsequent adjustments to the parameters as determined from Fig. 4 to optimize the fit. Our final choices are $C_{W1} = -4.0$ and $C_{W2} = 4.33$. From Eq. (36), the dependence of $\zeta$ on $x_1$ along the plait-point locus is obtained. In place of $C$, we choose values of $x_0 = 0.1$ and $\zeta_1 = 0.1$ so that $\zeta(x_0) = \zeta_1$.

Our final correlation is shown in Fig. 4 with the choices of adjustable parameters listed in Table I. The correlation achieves most, but not all, of our stated goals. The model describes LLE as shown by the large filled circles in reasonable agreement with the predictions of NIST14, which, we emphasize, are not actual experimental data. The model dew curves at 182 and 179 K, although differing somewhat from the coexisting vapor composition predictions of NIST14, are continuous (no spurious vapor–vapor equilibrium) with discontinuous derivatives at the three-phase locus, and, at least for the 182 K isotherm, the direction of discontinuity agrees with the 180° rule.

**Table I.** Parameters of the Model for Carbon Dioxide + Methane

| Parameter | Value | Purpose |
|---|---|---|
| $C_H$ | −15 | Leung–Griffiths parameter; moves curves left and right |
| $C_X$ | 0.16 | Leung–Griffiths parameter; narrows or widens curves |
| $C_Z$ | −1.4 | Leung–Griffiths parameter; lets $C_H$ vary with $\zeta$ |
| $C_R$ | 2.0 | Leung–Griffiths parameter; rotates $T$–$\rho$ curves |
| $C_Y$ | 1.5 | Leung–Griffiths parameter; lets $C_X$ vary with $\zeta$ |
| $C_{W1}$ | 4 | Amplitude of excess width function |
| $C_{W2}$ | 4.33 | Decay rate of excess width function |
| $x_0$ | 0.1 | Value of $x$ at which $\zeta = \zeta_1$ |
| $\zeta_1$ | 0.1 | Value of $\zeta$ at which $x_1 = x_0$ |
| $C_L$ | 1.7 | Amplitude of LLE construct |
| $s_t$ | 1.867 | Scaling factor of $t$ for UCEP |
| $s_\zeta$ | 2.2 | Scaling factor of $\zeta$ for UCEP |
| $a$ | 0.009 | Transition range for stretching transformation |
| $C_{vc}$ | 22.0 | Amplitude of vapor density augmentation |
| $t_r$ | 0.3 | Scale factor for $t$ in vapor density augmentation |

Furthermore, all experimental bubble curves are accurately correlated. The model dew curves are in at least fair agreement with experiment for $T > 240$ K but clearly to the left of the experimental points for 203.15 K $< T <$ 230 K. Thus our construction does not exactly reproduce the quantatitave behavior of the thermodynamic potential in the region between the plait-point and the consolute-point loci, but the overall qualitative behavior, with theoretical critical exponents, is reproduced. A difficulty with the present example is that $t = -0.14$ at the UCEP, whereas we have traditionally restricted the model to the range $-0.1 < t < 0$. Thus, the LLE in the present example is somewhat outside the "near-critical" regime with respect to VLE.

We appreciate the desirability of minimizing the number of adjustable parameters, but present techniques for scaling-law models of complicated mixtures require many parameters. A similar number of parameters was required to describe VLE of water + sodium chloride even over a small range of composition [10]. Our starting point, the modified Leung–Griffiths model, contained six adjustable parameters (in addition to those required to fit the pure coexistence curves and plait-point locus). The first five of these, $C_H$, $C_X$, $C_Z$, $C_R$, and $C_Y$, are listed in Table I and are defined in previous work [7, 9]. The sixth, $H_1$, which modified the linear critical line condition in a simple polynomial manner, is replaced here by the parameters $C_{W1}$, $C_{W2}$, $x_0$, and $\zeta_1$ in the more complicated relations of Eqs. (36) and (37). The remaining parameters in Table I were defined earlier in the text. In this work, the parameters were determined by graphical

and visual methods, and no formal nonlinear optimization techniques with minimization of an objective function has yet been attempted, although such methods have been used for the modified Leung–Griffiths model with only VLE [10, 40].

## 7. CONCLUSIONS

To our knowledge, this work presents the first complete nonclassical description of the fluid phase boundaries of a Type 2 mixture. Although this model may seem complex, and some aspects of it are without fundamental theoretical justification, its advantage is that all phase transitions are described by nonclassical exponents, which may be of more importance for Type 2 than for Type 1 mixtures. In the LLE experimental literature, one often sees an ad hoc fit of the data to Eq. (2) with an exponent of one-third, but without any connection to a complete thermodynamic model.

Our initial model has several limitations that in the future should be corrected for general applicability. The consolute point locus is independent of pressure in the model, whereas (relatively weak) pressure dependence has been observed for such loci [41]. Because the LLE construct is independent of $h$ on the liquid side, the model predicts equal molar densities for the coexisting liquids, which is not true in general [42]. A thermodynamic potential with discontinuities in higher derivatives would lead to higher-order phase transitions, and this must be kept in mind with constructions such as Eq. (19). Perhaps most importantly, we have suppressed a spurious "vapor–vapor equilibrium" at the three-phase locus but not necessarily over all of the one-phase vapor region, and to do so probably will require some further $h$-dependence in $w_{\mathrm{LLE}}$. Also, the thermodynamic behavior around a critical end point has been analyzed in some detail by Fisher [43, 44], and to the extent possible, the model should comply with Fisher's analysis. Nevertheless, this work represents a promising step toward the solution of a complicated problem and, hopefully, can be refined incrementally as the modified Leung–Griffiths model has been refined in recent years [9].

We note that a new nomenclature for binary fluid mixtures, to replace that of Van Konynenburg and Scott [1], has recently been proposed [45]. Within that nomenclature, the mixture we have considered would be classified as $1^{P}l$ instead of Type 2. In future work, we plan to test the model on binary mixtures with experimentally observed LLE. The best candidate mixtures at present appear to be carbon dioxide + carbon disulfide [23], water + sulfur dioxide [24], and possibly ammonia + isooctane [42].

## ACKNOWLEDGMENTS

The author thanks Amy Olson for assistance with the determination of the three-phase locus of carbon dioxide + methane from NIST14. He acknowledges the late Graham Morrison for first suggesting that the failure of the modified Leung–Griffiths model to correlate VLE of carbon dioxide + methane might arise from "virtual" liquid–liquid equilibrium below the freezing locus. He also thanks Michael Moldover, Daniel Friend, and Sergei Kiselev for valuable suggestions and Olga Kiseleva for drafting Fig. 1. This work was supported in part by the Division of Chemical Sciences, Office of Basic Energy Sciences, Office of Energy Research, U.S. Department of Energy.

## REFERENCES

1. P. H. Van Konynenburg and R. L. Scott, *Phil. Trans. Roy. Soc. (London)* **298**:495 (1980).
2. D. Y. Peng and D. B. Robinson, *Ind. Eng. Chem. Fund.* **15**:59 (1976).
3. K. Knudsen, E. H. Stenby, and J. G. Andersen, *Fluid Phase Equil.* **93**:55 (1994).
4. J. M. H. Levelt Sengers, in *Supercritical Fluid Technology*, J. F. Ely and T. J. Bruno, eds. (CRC Press, Boca Raton, FL, 1991), p. 1.
5. S. S. Leung and R. B. Griffiths, *Phys. Rev. A* **8**:2670 (1973).
6. M. R. Moldover and J. S. Gallagher, *AIChE J.* **24**:267 (1978).
7. M. R. Moldover and J. C. Rainwater, *J. Chem. Phys.* **88**:7772 (1988).
8. J. C. Rainwater, NIST Tech. Note 1328 (1989).
9. J. C. Rainwater, in *Supercritical Fluid Technology*, J. F. Ely and T. J. Bruno, eds. (CRC Press, Boca Raton, FL, 1991), p. 57.
10. M. Yu. Belyakov, S. B. Kiselev, and J. C. Rainwater, *J. Chem. Phys.* **107**:3085 (1997).
11. J. M. H. Levelt Sengers, *Pure Appl. Chem.* **55**:437 (1983).
12. K. A. Johnson, *J. Chem. Thermodyn.* **20**:889 (1988).
13. J. J. De Pablo and J.M. Prausnitz, *Fluid Phase Equil.* **59**:1 (1990).
14. H. Cheng, M. A. Anisimov, and J. V. Sengers, *Fluid Phase Equil.* **128**:67 (1997).
15. R. B. Griffiths and J. C. Wheeler, *Phys. Rev. A* **2**:1047 (1970).
16. P. Schofield, *Phys. Rev. Lett.* **22**:606 (1969).
17. J. C. Rainwater and D. G. Friend, *Phys. Lett. A* **191**:431 (1994).
18. J. C. Wheeler, *J. Chem. Phys.* **61**:4474 (1974).
19. M. A. Anisimov, E. E. Gorodetskii, V. D. Kulikov, and J. V. Sengers, *Phys. Rev. E* **51**:1199 (1995).
20. V. L. Pokrovskii, *JETP Lett.* **17**:156 (1973).
21. F. W. Balfour, J. V. Sengers, M. R. Moldover, and J. M. H. Levelt Sengers, *Proc. Seventh Symp. Thermophys. Prop.* (ASME, New York, 1977), p. 786.
22. D. G. Friend and M. L. Huber, *Int. J. Thermophys.* **15**:1279 (1994).
23. W. E. Reiff, H. Roth, and K. Lucas, *Fluid Phase Equil.* **73**:323 (1992).
24. B. C. Spall, *Can. J. Chem. Eng.* **41**:79 (1963).
25. Y. Arai, G. Kaminishi, and S. Saito, *J. Chem. Eng. Jpn.* **4**:113 (1971).
26. T. A. Al-Sahhaf, Ph.D. thesis (Colorado School of Mines, Golden, 1981).
27. J. Davalos, W. R. Anderson, R. E. Phelps, and A. J. Kidnay, *J. Chem. Eng. Data* **21**:81 (1976).

28. S. C. Mraw, S.-C. Hwang, and R. Kobayashi, *J. Chem. Eng. Data* **23**:135 (1978).
29. S.-C. Hwang, H. Lin, P. S. Chappelear, and R. Kobayashi, *J. Chem. Eng. Data* **21**:493 (1978).
30. H. G. Donnelly and D. L. Katz, *Ind. Eng. Chem.* **46**:511 (1954).
31. T. A. Al-Sahhaf, E. D. Sloan, and A. J. Kidnay, *AIChE J.* **30**:867 (1984).
32. A. Kreglewski and K. R. Hall, *Fluid Phase Equil.* **15**:11 (1983).
33. M. S.-W. Wei, T. S. Brown, A. J. Kidnay, and E. D. Sloan, *J. Chem. Eng. Data* **40**:726 (1995).
34. S. B. Kiselev and J. C. Rainwater, *Fluid Phase Equil.* **141**:129 (1997).
35. B. Bian, Y. Wang, J. Shi, E. Zhao, and B. C. Y. Lu, *Fluid Phase Equil.* **90**:177 (1993).
36. H. Knapp, R. Doring, L. Oellrich, U. Plocker, and J. M. Prausnitz, *Vapor–Liquid Equilibria of Low-Boiling Substances* (DECHEMA, Frankfurt, Germany, 1982).
37. *NIST14 NIST Mixture Property Database* (National Institute of Standards and Technology, Gaithersburg, MD, 1993 ).
38. M. M. Miller and K. D. Luks, *Fluid Phase Equil.* **44**:295 (1989).
39. U. K. Im and F. Kurata, *J. Chem. Eng. Data* **16**:412 (1971).
40. J. C. Rainwater and J. J. Lynch, *Int. J. Thermophys.* **15**:1231 (1994).
41. N. Dahmen and G. M. Schneider, *Fluid Phase Equil.* **87**:295 (1993).
42. W. B. Kay and F. Warzel, *AIChE J.* **4**:296 (1958).
43. M. E. Fisher, *Physica A* **172**:77 (1991).
44. M. E. Fisher and M. C. Barbosa, *Phys. Rev. B* **43**:11177 (1991).
45. A. Bolz, U. K. Deiters, C. J. Peters, and T. W. de Loos, *Pure Appl. Chem.* **70**:2233 (1998).